Novel Filoviruses, Hantavirus, and Rhabdovirus in Freshwater Fish, Switzerland, 2017

Melanie M. Hierweger, Michel C. Koch, Melanie Rupp, Piet Maes, Nicholas Di Paola, Rémy Bruggmann, Jens H. Kuhn, Heike Schmidt-Posthaus,[1] Torsten Seuberlich[1]

European perch (*Perca fluviatilis*) are increasingly farmed as a human food source. Viral infections of European perch remain largely unexplored, thereby putting farm populations at incalculable risk for devastating fish epizootics and presenting a potential hazard to consumers. To address these concerns, we applied metatranscriptomics to identify disease-associated viruses in European perch farmed in Switzerland. Unexpectedly, in clinically diseased fish we detected novel freshwater fish filoviruses, a novel freshwater fish hantavirus, and a previously unknown rhabdovirus. Hantavirus titers were high, and we demonstrated virus in macrophages and gill endothelial cells by using in situ hybridization. Rhabdovirus titers in organ samples were low, but virus could be isolated on cell culture. Our data add to the hypothesis that filoviruses, hantaviruses, and rhabdoviruses are globally distributed common fish commensals, pathogens, or both. Our findings shed new light on negative-sense RNA virus diversity and evolution.

Aquaculture is the fastest growing sector in food production worldwide (*1*); innovative intensive production technologies, such as recirculating aquaculture systems (RAS), are becoming increasingly valuable for commercial fish production (*2*). Attempts are continually made to introduce new types of fish into aquaculture, to reduce overfishing of wild fish populations, and to satisfy the progressing consumer demand for diverse supply (*3*). One example is the adaptation of European perch (*Perca fluviatilis*; order Perciformes, family Percidae) to farming and the growing consumer interest in this fish (*4*). European perch are actinopterygiids that naturally inhabit slow-flowing rivers, lakes, or ponds in Europe and northern Asia. During the 19th century, they were introduced into Australia as angling fish, where they are now considered invasive, competing with native fish for food and space, preying on other fish, and breeding to overpopulation (*5*).

Although little is known about diseases affecting European perch in the wild, infectious diseases lead to high mortality among these fish in aquaculture, making farming of these fish economically challenging. One of the main threats is infection with perch rhabdovirus (PRV; family *Rhabdoviridae*, genus *Perhabdovirus*), leading to the central nervous system (CNS) signs of loss of equilibrium and aberrant swimming behavior and to higher mortality (*2*,*6*–*10*). Lack of investigation of the occurrence and diversity of other pathogenic virus infections of European perch that result in disease impairs the treatment, control, and prevention of disease outbreaks in farm populations. To address this knowledge gap, we applied virus diagnostics, including metatranscriptomics (study of gene expression of microbes in natural environments), to a set of samples collected from sick juvenile European perch at a perch farm in Switzerland in 2017. Although we did not find PRV in these fish, our investigation led to the discovery of 5 novel negative-sense RNA viruses, belonging to the negarnaviricot families *Rhabdoviridae*, *Filoviridae*, and *Hantaviridae*, that could possibly contribute to disease development.

Methods

European Perch Origin

The European perch used in this study were raised in a private pond in Saxony, Germany, and were exported to a farm that uses RAS in Bernese Oberland,

Author affiliations: University of Bern, Bern, Switzerland (M.M. Hierweger, M.C. Koch, M. Rupp, R. Bruggmann, H. Schmidt-Posthaus, T. Seuberlich); KU Leuven, Leuven, Belgium (P. Maes); US Army Medical Research Institute of Infectious Diseases, Frederick, Maryland, USA (N. Di Paola); Integrated Research Facility at Fort Detrick, Frederick (J. H. Kuhn)

DOI: https://doi.org/10.3201/eid2712.210491

[1]These authors contributed equally to this article.

Switzerland, at 16 g (≈11,200 fish) and 33 g (≈4,800 fish). Eleven live juvenile European perch were sent to the Centre for Fish and Wildlife Health (FIWI), University of Bern (Bern, Switzerland), where they were euthanized and subjected to microbiological (including parasitologic, bacteriologic, mycologic, and virologic) and pathologic (including histopathologic) examination. Because the remaining fish at the farm exhibited clinical signs of disease, they were kept in quarantine for an additional 2 months and subsequently euthanized.

Cell Culture

We used bluegill (*Lepomis macrochirus*) fry cells (BF-2) and fathead minnow (*Pimephales promelas*) epithelioma papulosum cyprini (EPC) cells. These cells were originally obtained from the Friedrich-Loeffler-Institute, Federal Research Institute for Animal Health (Greifswald-Insel Riems, Germany; Collection of Cell Lines in Veterinary Medicine, catalog nos. CCLV-RIE 290 and CCLV-RIE 173 are maintained at FIWI).

We inoculated the cells with small pieces of pooled CNS or spleen, kidney, heart, and pyloric ceca tissue from 5 of the 11 euthanized European perch (in total <5 g) and incubated at 15°C. We monitored the cell cultures for CPE daily for 7 days by using light microscopy and then monitored subcultures for another 7 days. We harvested supernatants from cell cultures showing CPE and tested by reverse transcription PCR (RT-PCR) for the common European perch pathogen PRV, targeting the glycoprotein (*G*) gene of PRV isolate 9574.1 (GenBank accession no. JF502613), according to a previously published protocol, by using the primer pair oPVP116/118 and oPVP126/Rha2 (*11*).

High-Throughput Sequencing and Bioinformatics

We extracted total RNA from fresh-frozen pooled visceral organs and CNS tissue, originally taken for cell culture inoculation by using TRI Reagent (Sigma Life Sciences, https://www.sigmaaldrich.com), according to the manufacturer's instructions. We then prepared a high-throughput sequencing (HTS) library with the TruSeq Stranded Total RNA kit (Illumina, https://www.illumina.com) and performed HTS on a HiSeq 3000 machine (Illumina), generating paired-end reads of 2 × 150 bp. We performed bioinformatic analysis as described previously (*12*) (Appendix, https://wwwnc.cdc.gov/EID/article/27/12/21-0491-App1.pdf).

Reverse Transcription PCR, Rapid Amplification of cDNA Ends, and Sanger Sequencing

To fill gaps between HTS scaffolds, we reverse-transcribed extracted RNA to cDNA, performed PCRs, and subjected the amplicons to Sanger sequencing (Appendix). We performed 3′ and 5′ rapid amplification of cDNA ends (RACE), as described previously, on RNA extracted from pooled organs and CNS tissue as well as cell culture supernatants (*13*) (Appendix).

Taxonomic Analyses

We performed taxonomic analyses by using protein or nucleic acid sequences, following precedents established by the International Committee on Taxonomy of Viruses (ICTV) *Filoviridae* (*14*,*15*), *Hantaviridae* (*16*), and *Rhabdoviridae* (*17*) Study Groups. New filovirus-like genome sequences were analyzed by using pairwise sequence comparison (*18*) and maximum-likelihood phylogenetics. Filovirus phylogenetic estimations were inferred in FastTree version 2.1 (*19*) by using a general time-reversible model with 20 gamma-rate categories, 5,000 bootstrap replicates, and exhaustive search parameters (-slow) and pseudocounts (-pseudo). The new rhabdovirus-like sequence was taxonomically placed via analysis of its full-length large protein gene (*L*) sequence using maximum-likelihood phylogenetics. We applied the maximum-likelihood method in MEGA X (*20*) with 1,000 bootstraps for rhabdovirus and hantavirus phylogenetic estimations.

Histopathology and In Situ Hybridization

During a complete necropsy of the 11 fish, we used 3 whole perch for histologic examination. We fixed these fish in 10% buffered formalin for 24 hours and embedded cut sections of the gills, longitudinal head sections, and longitudinal cut sections of the body cavity in paraffin. We prepared 3-µm sections and stained them with hematoxylin and eosin according to standard protocols. We conducted chromogenic in situ hybridization on all formalin-fixed paraffin-embedded (FFPE) tissues used for histopathology. We performed staining with the RNAscope system (Advanced Cell Diagnostics, https://acdbio.com) (Appendix).

Results

Clinical and Pathologic Findings

In December 2016, a total of 16,000 juvenile European perch were imported from Saxony, Germany, to a farm using RAS in Bernese Oberland, Switzerland. After arrival, the fish were routinely quarantined. Shortly after arrival, because of a high death rate of 1% per day (reference range 0.01%–0.03% per day), 11 randomly selected live fish were sent to FIWI for microbiological and pathologic examination. Clinical signs included anorexia, lethargy, skin ulcerations, multifocal hemorrhages, and eroded tail fins. Culture and PCR indicated that skin ulcerations were caused by oomycete (*Saprolegnia parasitica*) infection (*21*). Histopathology revealed mild to moderate gill epithelial proliferation and epithelial cell hypertrophy. Additional findings included necrotizing dermatitis with hemorrhage and intralesional oomycete hyphi and bacterial colonies. The newly arrived fish were treated with flubendazole, formalin, and peracetic acid, but death increased to 1.8%–4.2% per day. Two months after importation, deaths for the quarantined fish reached 22%–27% in total. All remaining fish were euthanized and discarded, thereby preventing these fish from entering the food chain.

Virus Isolation

For routine virus investigation, we exposed standard fish cell cultures (BF-2 and EPC) to suspensions of pooled perch CNS and pooled visceral organs. We selected these cell lines because of their high susceptibility to diverse fish viruses (*22*). CPE developed 10 days after inoculation of CNS suspension into BF-2 cells and 13 days after inoculation into EPC cells. Affected cell supernatants were harvested and tested preliminarily positive for PRV infection by RT-PCR. The sequence of the detected amplicon was, however, only 78% identical to the sequence of the perhabdovirus lake trout rhabdovirus (LTRV; GenBank accession no. AF434991), indicating the presence of a perhabdovirus distinct from PRV/LTRV.

Novel Perhabdovirus

To further characterize the putative novel perhabdovirus, we performed metatranscriptomics by using HTS and bioinformatic analysis of pooled CNS tissue and visceral organ RNA extracts of 5 fish. We found 16 sequence scaffolds 247–1,454-nt long with mean k-mer coverages of 1.0–5.9 and nucleotide sequence identities of 62%–98% to perhabdovirus genomes (Appendix Table 1). We mapped these scaffolds to LTRV (GenBank accession no. AF434991) and PRV (GenBank accession no. JX679246) as references and closed sequence gaps by RT-PCR and RACE followed by Sanger sequencing. The resulting complete genome of the novel virus was 11,595-nt long and had the characteristic genomic organization of (pe)rhabdoviruses (Figure 1, panel A). Each of the open reading frames (ORFs) is flanked by conserved transcriptional initiation (3′-UUGUUC) and termination/polyadenylation (3′-AURC$[U]_7$) signals with inverse complementarity of 13 nt of the 3′ and 5′ terminal genome sequences.

Phylogenetic comparison of the *L* gene confirmed a close relationship of the new virus to the 2 members of the species *Sea trout perhabdovirus* (i.e., LTRV and Swedish sea trout virus; GenBank accession no. AF434992) (Figure 1, panel B) and a recently described and thus far unclassified virus from a percid (sea trout rhabdovirus isolate 18/203; GenBank accession no. MN963997). This relationship is also reflected in phylogenetic comparisons of the nucleoprotein (*N*), phosphoprotein (*P*), matrix protein (*M*), and *G* genes (Appendix Figure 1). The current perhabdovirus sequence-based species demarcation criterion is a minimum divergence of 15% in the *L* gene (*17*). The *L* gene sequence of the novel virus is most closely related to that of the isolate 18/203 (divergence 10%); *L* genes of both viruses are ≈19% divergent from the next closest related perhabdovirus, sea trout perhabdovirus isolate R6146 (GenBank accession no. MN963999), thus indicating that we discovered a novel perhabdovirus that should be assigned to a new species along with isolate 18/203. We named the new virus Egli virus (EGLV) after a local Swiss-German word for European perch and deposited the complete viral genome sequence into GenBank (accession no. MN510774). Detection of EGLV in European perch FFPE tissue sections by RNA in situ hybridization was unsuccessful.

Four Novel Filoviruses

In addition to scaffolds that ultimately led us to identify EGLV, we found 41 scaffolds 240–4,726-nt long with low k-mer coverage (0.8–4.8×). The deduced amino acid sequences were 28%–30% identical to proteins of Huángjiāo virus (HUJV), a recently identified virus of marine greenfin horse–faced filefish (*Thamnaconus septentrionalis*) captured in the East China Sea (*23*) (Appendix Table 1). Alignment of these scaffolds to the HUJV genome (GenBank accession no. MG599981) and the deduced amino acid sequences to those of HUJV-encoded proteins revealed a complex scenario suggesting the presence of several distinct thamnoviral genomes, however with numerous gaps between the scaffolds. To obtain complete or coding-complete viral genome sequences, we resequenced the HTS library to generate ≈10 times more paired-end reads (2,051,046,671) than during the initial HTS run, reassembled the sequences, and performed RT-PCR and Sanger sequencing to bridge sequence gaps. This effort resulted in 3 long scaffolds of 13,764 nt (k-mer coverage 24×), 14,593 nt (k-mer coverage 15×), and 13,066 nt (k-mer coverage 5×), corresponding to 3 novel viruses.

We named these viruses Fiwi virus (FIWIV; GenBank accession no. MN510772), after FIWI; Oberland virus (OBLV;) GenBank accession no. MN510773), after Bernese Oberland; and Kander virus (KNDV;

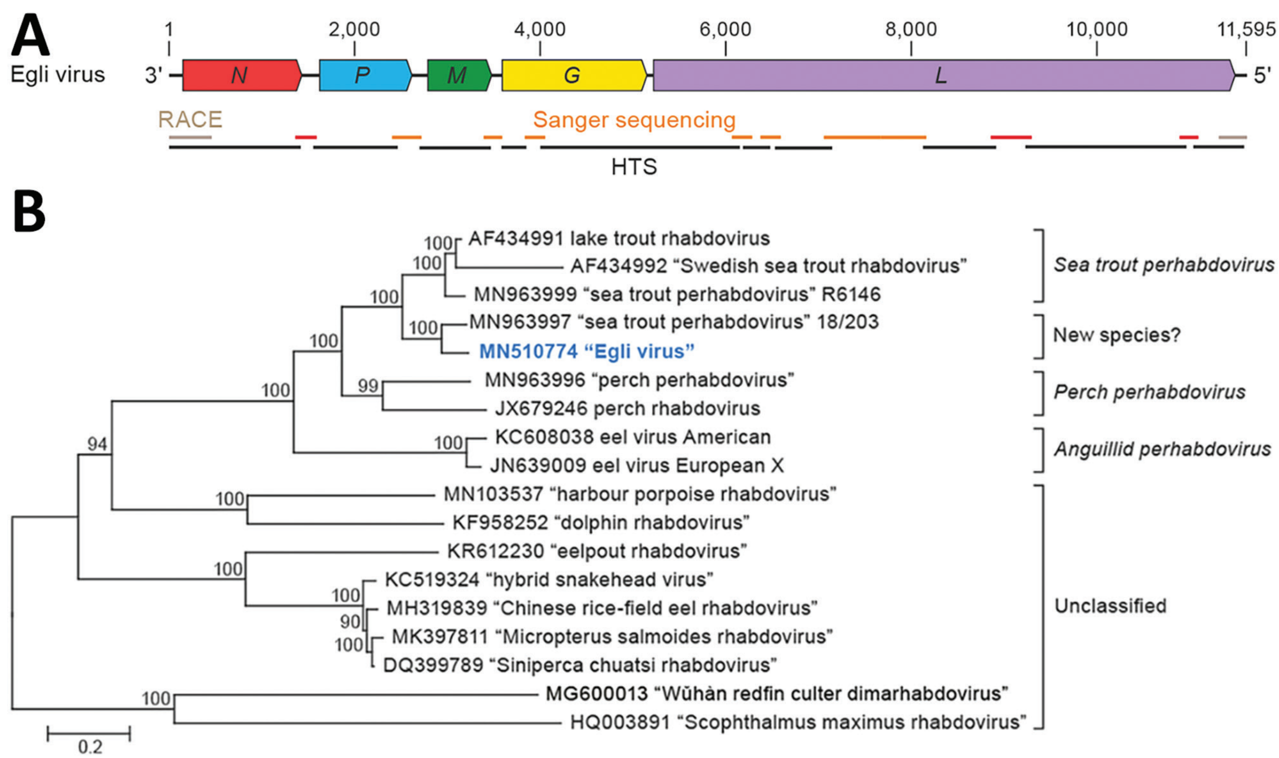

Figure 1. Identifying a novel rhabdovirus in European perch. A) Schematic representation of the Egli virus genome organization; open reading frames are indicated by colored arrows. B) Maximum-likelihood phylogenetic tree of the nucleotide sequence of the Egli virus *L* gene (bold blue) and representative classified and unclassified members of the genus *Perhabdovirus.* Numbers near nodes on the trees indicate bootstrap values. Branches are labeled by GenBank accession number, virus name, and virus name abbreviation in parenthesis. Names of unclassified likely perhabdoviruses are placed in quotation marks and printed without name abbreviations. Scale bar indicates number of substitutions per site, reflected by branch lengths. *G*, glycoprotein gene; HTS, high-throughput sequencing; *L*, large protein gene; *M*, matrix protein gene; *N*, nucleoprotein gene; *P*, phosphoprotein gene; RACE, rapid amplification of cDNA ends.

GenBank accession no. MW093492), after the Kander River, which flows through Bernese Oberland. Whereas the FIWIV genome appears to be coding complete, the sequences of OBLV are coding incomplete at the 5′ terminus and of KNDV at both the 5′ and the 3′ termini. All attempts to determine the authentic 3′ and 5′ termini by RACE were unsuccessful, most likely because of low viral RNA loads. However, all 3 sequences have the genomic features of HUJV, encoding the filovirus-typical proteins nucleoprotein (NP), polymerase cofactor (VP35), glycoprotein ($GP_{1,2}$), transcriptional activator (VP30), and large protein (L) containing an RNA-directed RNA polymerase (RdRp) domain, as well as 1–2 novel proteins (*14*,*23*,*24*) (Figure 2, panel A). Phylogenetic comparison of the FIWIV, OBLV, and KNDV genomic sequences (Figure 2, panel B) and *L* gene sequences with those of representative classified viruses of the family *Filoviridae* (Figure 2, panel C) confirmed the genetic relationship of all 3 viruses to HUJV. The current demarcation criteria for filovirus sequence-based genus and species are ≥55% and ≥23% sequence divergence over complete genome sequences determined by using pairwise sequence comparison (*14*,*15*). We found a pairwise divergence of 49% compared with HUJV by using the FIWIV genome sequence (Table), indicating that FIWIV is a member of a new thamnovirus species ("Thamnovirus percae"). The available KNDV genome sequence is 49% divergent from HUJV and 37% divergent from FIWIV (Table), suggesting that KNDV represents yet another novel thamnovirus species ("Thamnovirus kanderense"). In contrast, OBLV was >62% divergent from HUVJ, FIWIV, and KNDV viruses and thus represents a new species ("Oblavirus percae") within a new genus ("Oblavirus"). All attempts to detect FIWIV or OBLV viruses in 3 European perch FFPE tissue sections were unsuccessful.

In addition to FIWIV, OBLV, and KNDV, we found 4 shorter scaffolds (573–3,259 nt; Appendix Figure 2) similar to various HUJV genes, but attempts to demonstrate a physical linkage of these sequences by RT-PCR were not successful. Still, the presence of these scaffolds is indicative of at least 1 additional novel filovirus, which we were not able to further characterize.

Novel Hantavirus

In the same RNA extract of pooled organs, we found 3 scaffolds, of which the deduced amino acid sequences

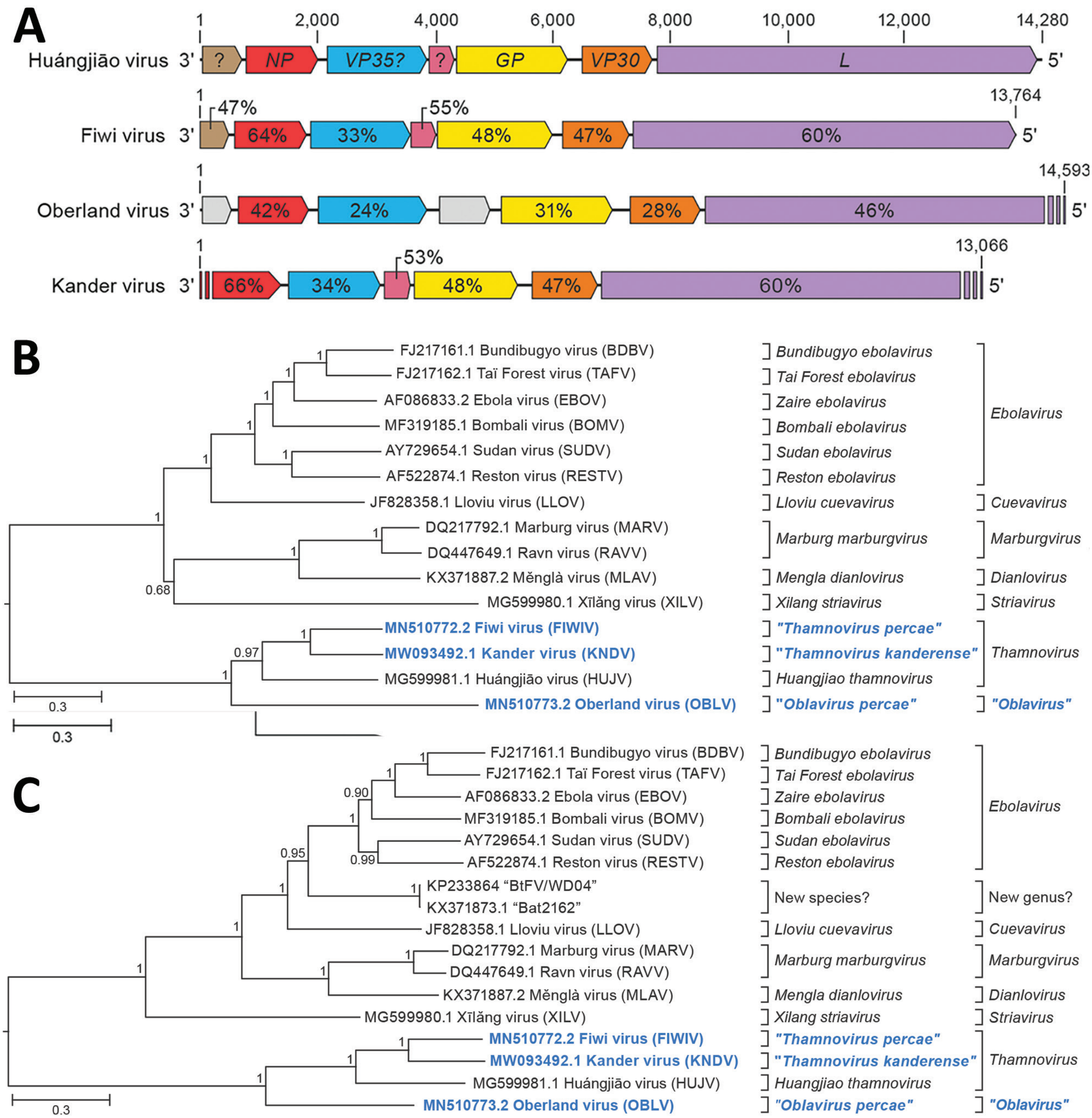

Figure 2. Identifying 3 novel filoviruses in European perch. A) Schematic representation of the genome organization of Fiwi virus, Oberland virus, and Kander virus compared with Huángjiāo virus (HUJV). Open reading frames (ORFs) are indicated by colored arrows. ORFs encoding HUJV-like proteins (indicated as percentages) are depicted by the same color. Undetermined ORF starts and ends are shown as stripes. B, C) Maximum-likelihood phylogenetic trees of the new filovirus genome sequences (bold blue) generated by using coding-complete and near-complete genome sequences (B) or only *L* gene sequences (C) of representative members of the family *Filoviridae*. Numbers near nodes on the trees indicate bootstrap values. Branches are labeled by GenBank accession number and virus names. Scale bar indicates number of substitutions per site, reflected by branch lengths. *GP*, glycoprotein gene; *L*, large protein gene; *NP*, nucleoprotein gene; *VP30*, transcriptional activator gene; *VP35*, polymerase cofactor gene.

were 25%–35% similar to those of the large (L), medium (M), and small (S) segments of Wēnlǐng minipizza batfish virus (WEMBV) and Wēnlǐng red spikefish virus (WERSV). WEMBV was recently identified in apparently healthy minipizza batfish (*Halieutaea stellate*) and WERSV in red spikefish (*Triacanthodes anomalus*) captured in the East China Sea (Appendix Table 1) (*23*). The mean k-mer coverage of these scaffolds ranged from 3×10^3 to 1.5×10^4, indicating a high viral RNA load. Using Sanger sequencing and RACE, we determined the complete sequences of the genomic L (GenBank accession no. MN510769), M (GenBank accession no. MN510770), and S (GenBank accession no. MN510771) segments of a novel virus, here named Bern perch virus. Similar to WEMBV and WERSV, the Bern perch virus L segment (6,372 nt) was deduced to encode the L protein including an RdRp domain, the M segment (3,804 nt) was deduced to encode the glycoprotein precursor, and the S segment (2,435 nt) was deduced to encode the nucleocapsid protein (Figure 3, panel A). The S and M segments contain 2 additional ORFs encoding putative proteins not represented in current protein databases in antisense (S segment) and sense (M segment) orientation. Alignment of the 3′ and 5′ sequences of all 3 segments revealed that the 8 terminal nucleotides are complementary within and conserved among segments (Figure 3, panel B), a known feature of members of the order *Bunyavirales* (*25*). However, these terminal sequences differ from those of members of the genus *Orthohantavirus* and are similar to those of members of the genus *Orthobunyavirus* (Appendix Table 1). Phylogenetic analysis of the L protein confirmed the close relationship of Bern perch virus (BPV) to all currently classified actinoviruses (Figure 3, panel C; Appendix Figure 3) but indicated the need for a novel species to accommodate this virus. This need was confirmed by DEmARC (Diversity Partitioning by Hierarchical Clustering) analysis (*26*); on the basis of this evidence, the ICTV officially established this species as *Perch actinovirus* in 2021 (*27*,*28*).

Using in situ hybridization on FFPE tissue sections, we were able to detect BPV genomic RNA in gills with histopathologic lesions of 2 fish (Figure 4, panels A, B; Appendix Figure 4) and in a granuloma in the perivisceral fat tissue of 1 of these animals. Morphologically, we identified the affected cells in the gills and the perivisceral fat tissue as putative macrophages. In addition, putative endothelial cells were labeled positively in the gills (Figure 4, panel B).

Discussion

The diversity of fish viruses, in particular that of RNA viruses, remains poorly understood (*29*). Recent initial studies indicate that this diversity is enormous and that many viral taxa that have been established for pathogens of humans and other mammals need to be redefined (*23*,*30*–*32*). Husbandry conditions in huge tanks used on farms may favor the emergence and rapid intraspecies and interspecies transmission of fish viruses, potentially resulting in high economic loss for the fish industry. Also of concern is the introduction of novel viruses from fish farms into native fauna, which could have disastrous ecologic consequences. In addition, viruses of unknown pathogenicity in food animals may have zoonotic potential of yet unpredictable importance.

In this study, we identified 1 novel rhabdovirus, 4 novel filoviruses (3 confirmed and 1 likely), and 1 novel hantavirus in morbid farmed European perch. The discovery of a novel rhabdovirus was not surprising and adds to the role of rhabdoviruses in fish health; rhabdoviruses, in particular those of the genera *Novirhabdovirus*, *Perhabdovirus*, *Sprivivirus*, and *Vesiculovirus*, are notorious marine and freshwater fish pathogens, causing diseases characterized by high lethality (*33*,*34*). Thus, these viruses pose a considerable threat to aquaculture. The European perch examined in this study exhibited signs compatible with rhabdovirus infection (*7*). Using HTS and exposing cell cultures to CNS tissue suspensions, we discovered a novel perhabdovirus, Egli virus. Although the viral RNA loads in tissues were low and we could not detect RNA by in situ hybridization in tissue sections, we were able to isolate the virus from brain tissue. Rhabdoviruses in perch are usually associated with disease and not known as commensals. The host range of Egli virus is unknown, but genetically it is more closely related to viruses identified in trout than to those infecting perch, suggesting the possibility of cross-species transmission, highlighting a concern for farms that raise fish other than perch and for native fish populations. Discovery of a lake trout rhabdovirus

Table. Pairwise distances of complete or coding-complete genome nucleotide sequences between the newly identified Fiwi virus, HUJV, and the closest related mammalian filovirus, BOMV*

Virus	Fiwi virus	Oberland virus	Kander virus	HUJV
Oberland	66%			
Kander	37%	62%		
HUJV	49%	64%	49%	
BOMV	86%	87%	87%	86%

*Fiwi virus, GenBank accession no. MN510772. Oberland (GenBank accession no. MN510773) and Kander (GenBank accession no. MW093492) virus sequences are not coding complete and were compared on the basis of the available incomplete sequences. BOMV, Bombali virus (GenBank accession no.MK340750); HUJV, Huángjiāo virus.

as a probable cause of disease in European perch in Ireland (*7*) supports the hypothesis of high potential for interspecies transmission of these viruses.

Unexpectedly, we were able to assemble near-complete viral genomes of 3 novel filoviruses (Fiwi, Oberland, and Kander viruses) and detected a likely fourth filovirus in the diseased perch. Until recently, filoviruses, notorious for causing disease in humans with extremely high lethality (*35*), were thought to exclusively infect mammals. This view changed with the discovery of Xīlǎng virus (the only member of genus *Striavirus*) in striated frogfish (*Antennarius striatus*) and HUJV in greenfin horse-faced filefish captured in the East China Sea (*23*) as well as apparent thamnoviruses John Dory filovirus in John Dory fish (*Zeus faber*) and blue spotted goatfish filovirus in blue spotted goatfish (*Upeneichthys lineatus*) purchased at a fish market in Sydney, New

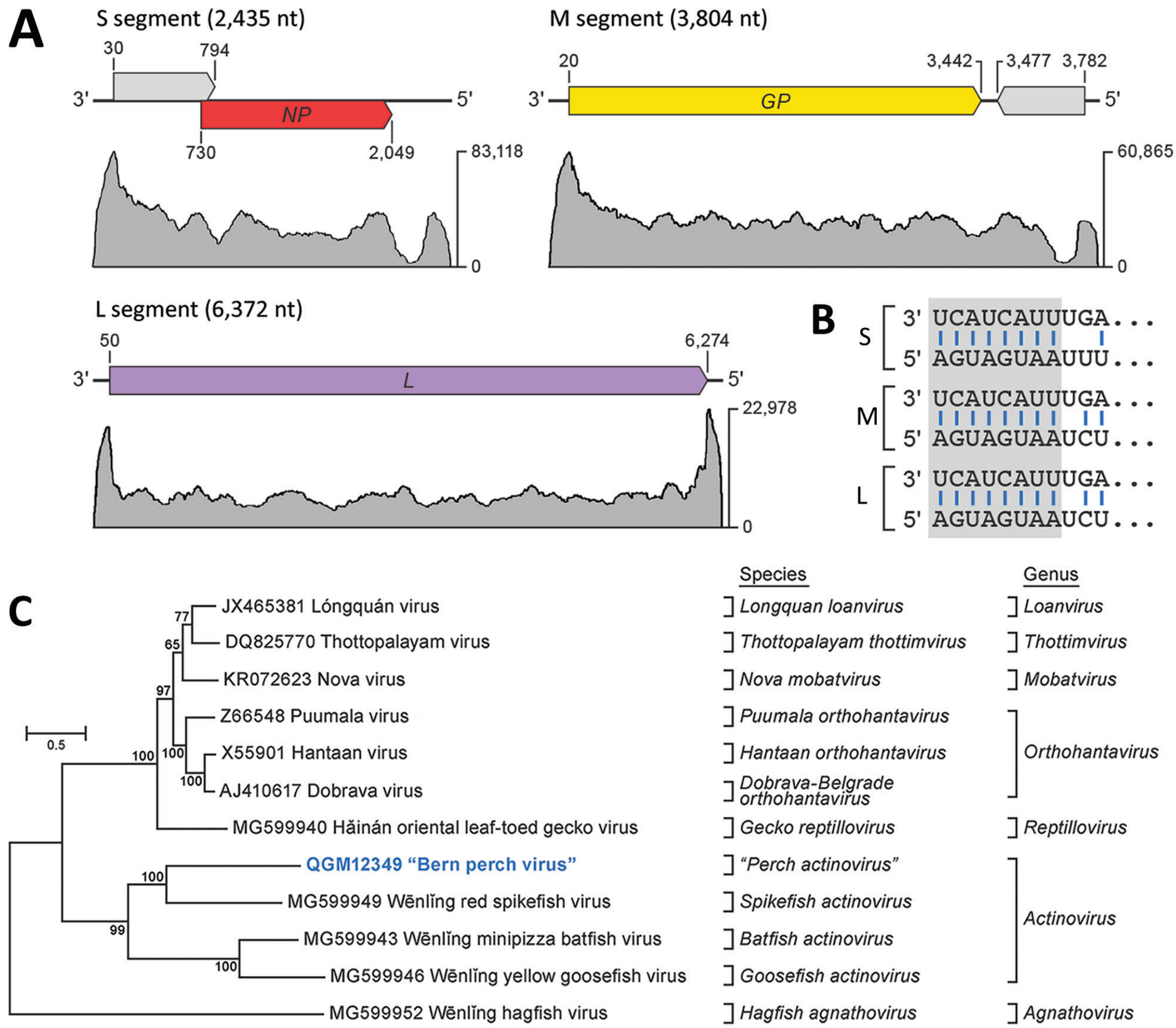

Figure 3. Identifying a novel hantavirus in European perch. A) Schematic representation of the 3 genome segments of Bern perch virus; open reading frames are indicated as colored arrows. Coverage plots of high-throughput sequencing reads are shown for each segment, and maximum-read coverages are indicated on the right. B) Alignment of the terminal sequences (11 nt) of the 3 segments. The terminal 8 nucleotides (gray box) are complementary within and conserved among segments. C) Maximum-likelihood phylogenetic tree of the Bern perch virus RNA-directed RNA-polymerase amino-acid sequence (bold blue) with RNA-directed RNA-polymerase amino-acid sequences of representative members of the family *Hantaviridae.* Numbers near nodes on the trees indicate bootstrap values. Branches are labeled by GenBank accession number, and virus name. Scale bar indicates number of substitutions per site, reflected by branch lengths. *GP*, glycoprotein gene; L, large; M, medium; *NP*, nucleocapsid protein gene; S, small.

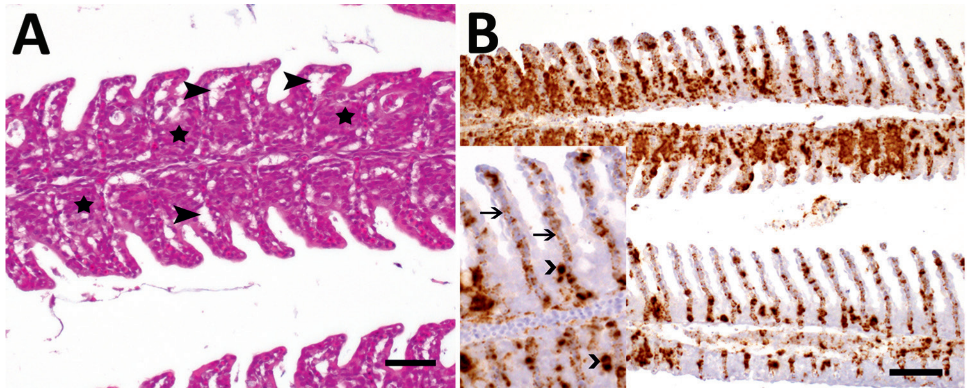

Figure 4. Histopathologic lesions and viral RNA in European perch infected with Bern perch virus. A) Histopathologic lesions in gills (hematoxylin and eosin stain) showing epithelial hypertrophy and hyperplasia, multifocally leading to lamellar fusion (stars) and multifocal epithelial lifting due to edema (closed arrowheads). Scale bar indicates 25 μm. B) In situ hybridization detection of RNA in gills (brown labeling): brown perch virus positive macrophages, more pronounced in proliferated areas, and endothelial cells. Inset: higher magnification showing positive macrophages (open arrowheads) and endothelial cells (arrows with open heads). Scale bar indicates 50 μm.

South Wales, Australia (*31*). However, currently, <300 nt contigs are known from John Dory fish and blue spotted goatfish filoviruses; hence, their true taxonomic affiliation remains to be determined. In contrast to Xīlǎng virus, HUJV, John Dory filovirus, and blue spotted goatfish filovirus (all of which were found in marine fish in China and Australia), FIWIV, OBLV, and KNDV apparently infect freshwater fish in Europe. This geographic and ecologic distribution indicates that filoviruses are broadly dispersed fish commensals or potential pathogens that probably number in the hundreds or thousands. Although on the basis of our data we cannot attribute filovirus infection to individual fish, a possible scenario includes co-infection with FIWIV, OBLV, KNDV, EGLV, or BPV or any combination of these viruses. Thamnovirus abundance was low in the sampled European perch, and detection of thamnoviral genomic RNA proved impossible in FFPE tissues. This low abundance, together with the unsuccessful attempt to demonstrate viral RNA in the tissue, suggests that infection in the investigated fish was subclinical rather than the cause of the observed clinical signs.

We also identified a novel hantavirus, BPV. Hantaviruses are best known as rodent-borne viruses of the mammantavirin genus *Orthohantavirus*, which cause hemorrhagic fever with renal syndrome or hantavirus pulmonary syndrome in humans (*36*) but have also been found in bats and eulipotyphla. Reptile hantaviruses (family *Repantavirinae*, genus *Reptillovirus*) and fish hantaviruses (family *Actantavirinae*, genus *Actinovirus*, and family *Agantavirinae*, genus *Agnathovirus*) (*32*) have only recently been discovered. The fish viruses include the actinoviruses WEMBV, WERSV (*23*), and Wēnlǐng yellow goosefish virus (detected in yellow goosefish [*Lophius litulon*] captured in China [*23*]); the likely actinovirus Aronnax virus, found in pygmy goby (*Eviota zebrina*) purchased at a fish market in Sydney (*31*); and the agnathovirus Wēnlǐng hagfish virus, detected in inshore hagfish (*Eptatretus burgeri*) captured in China (*23*). Similar to our filovirus findings, the discovery of BPV is remarkable because this actinovirus was found in freshwater fish from Europe rather than in marine fish from China or Australia. Actinoviruses have not yet been associated with disease in fish. Using in situ hybridization, we demonstrated, however, high concentrations of BPV RNA in macrophages and endothelial cells in the gills as well as in macrophages in the perivisceral fat tissue of morbid European perch. Other cell types tested negative. Human pathogenic orthohantaviruses predominantly infect macrophages and microvascular endothelial cells of a variety of organs, which leads to increased vascular permeability and severe disease (*11*). It is therefore tempting to speculate that the pathology observed in the gills of the European perch may have resulted in dyspnea, contributing to elevated mortality. In conclusion, our identification of new rhabdoviruses, filoviruses, and hantaviruses in farmed European perch in Switzerland raises concerns about the global distribution, host spectrum, and risks to human and animal health for these viruses.

Acknowledgments

We thank Pamela Nicholson and the HTS platform, University of Bern, for performing the HTS runs, Elsbeth Keller-Gautschi and Regula Hirschi for excellent technical assistance, and Laurent Bigarré for scientific exchange and advice. We are grateful to Anya Crane for editing the manuscript.

This work was supported by the Swiss National Science Foundation (grant no. 31003A_163438 to R.B. and T.S.), the Swiss Food Safety and Veterinary Office (grant no. MON-108 to T.S.), and the Swiss Innovation Agency (Innossuisse, grant no. 25178.1 PFLS-LS to H.S.-P). This work was supported in part through Laulima Government Solutions, LLC, prime contract with the US National Institute of Allergy and Infectious Diseases under contract no. HHSN272201800013C. J.H.K. performed this work as an employee of Tunnell Government Services, a subcontractor of Laulima Government Solutions, LLC, under contract no. HHSN272201800013C.

HTS raw data from this study have been deposited into the Sequence Read Archive (https://www.ncbi.nlm.nih.gov/sra) as SRR12586223.

About the Author

Dr. Hierweger works as a postdoctoral researcher at the Division of Neurological Sciences, Vetsuisse Faculty, University of Bern. Her main research interest is the discovery of emerging viruses and their involvement in disease.

References

1. Food and Agriculture Organization of the United Nations. The state of world fisheries and aquaculture 2018. Meeting the sustainable development goals [cited 2021 Jul 10]. http://www.fao.org/3/i9540en/I9540EN.pdf
2. Martins CIM, Eding EH, Verdegem MCJ, Heinsbroek LTN, Schneider O, Blancheton JP, et al. New developments in recirculating aquaculture systems in Europe: a perspective on environmental sustainability. Aquacult Eng. 2010;43:83–93. https://doi.org/10.1016/j.aquaeng.2010.09.002
3. Naylor RL, Hardy RW, Buschmann AH, Bush SR, Cao L, Klinger DH, et al. A 20-year retrospective review of global aquaculture. Nature. 2021;591:551–63. https://doi.org/10.1038/s41586-021-03308-6
4. Policar T, Schaefer FJ, Panana E, Meyer S, Teerlinck S, Toner D, et al. Recent progress in European percid fish culture production technology—tackling bottlenecks. Aquacult Int. 2019;27:1151–74. https://doi.org/10.1007/s10499-019-00433-y
5. Morgan DL, Gill HS, Maddern MG, Beatty SJ. Distribution and impacts of introduced freshwater fishes in Western Australia. N J Mar Freshwater Res. 2004;38:511–23. https://doi.org/10.1080/00288330.2004.9517257
6. Caruso C, Gustinelli A, Pastorino P, Acutis PL, Prato R, Masoero L, et al. Mortality outbreak by perch rhabdovirus in European perch (*Perca fluviatilis*) farmed in Italy: clinical presentation and phylogenetic analysis. J Fish Dis. 2019;42:773–6. https://doi.org/10.1111/jfd.12975
7. Ruane NM, Rodger HD, McCarthy LJ, Swords D, Dodge M, Kerr RC, et al. Genetic diversity and associated pathology of rhabdovirus infections in farmed and wild perch *Perca fluviatilis* in Ireland. Dis Aquat Organ. 2014;112:121–30. https://doi.org/10.3354/dao02801
8. Rupp M, Knüsel R, Sindilariu P-D, Schmidt-Posthaus H. Identification of important pathogens in European perch (*Perca fluviatilis*) culture in recirculating aquaculture systems. Aquacult Int. 2019;27:1045–53. https://doi.org/10.1007/s10499-019-00382-6
9. Dorson M, Torchy C, Chilmonczyk S, Kinkelin P, Michel C. A rhabdovirus pathogenic for perch, *Perca fluviatilis* L.: isolation and preliminary study. J Fish Dis. 1984;7:241–5. https://doi.org/10.1111/j.1365-2761.1984.tb00929.x
10. Dannevig BH, Olesen NJ, Jentoft S, Kvellestad A, Taksdal T, Håstein T. The first isolation of a rhabdovirus from perch (*Perca fluviatilis*) in Norway. Bull Eur Assoc Fish Pathol. 2001;21:186–94.
11. Noack D, Goeijenbier M, Reusken CBEM, Koopmans MPG, Rockx BHG. Orthohantavirus pathogenesis and cell tropism. Front Cell Infect Microbiol. 2020;10:399. https://doi.org/10.3389/fcimb.2020.00399
12. Kauer RV, Koch MC, Hierweger MM, Werder S, Boujon CL, Seuberlich T. Discovery of novel astrovirus genotype species in small ruminants. PeerJ. 2019;7:e7338. https://doi.org/10.7717/peerj.7338
13. Hierweger MM, Werder S, Seuberlich T. Parainfluenza virus 5 infection in neurological disease and encephalitis of cattle. Int J Mol Sci. 2020;21:498. https://doi.org/10.3390/ijms21020498
14. Kuhn JH, Amarasinghe GK, Basler CF, Bavari S, Bukreyev A, Chandran K, et al.; ICTV Report Consortium. ICTV virus taxonomy profile: *Filoviridae*. J Gen Virol. 2019;100:911–2. https://doi.org/10.1099/jgv.0.001252
15. Bào Y, Amarasinghe GK, Basler CF, Bavari S, Bukreyev A, Chandran K, et al. Implementation of objective PASC-derived taxon demarcation criteria for official classification of filoviruses. Viruses. 2017;9:106. https://doi.org/10.3390/v9050106
16. Laenen L, Vergote V, Calisher CH, Klempa B, Klingström J, Kuhn JH, et al. *Hantaviridae*: current classification and future perspectives. Viruses. 2019;11:788. https://doi.org/10.3390/v11090788
17. Walker PJ, Blasdell KR, Calisher CH, Dietzgen RG, Kondo H, Kurath G, et al.; ICTV Report Consortium. ICTV virus taxonomy profile: *Rhabdoviridae*. J Gen Virol. 2018;99:447–8. https://doi.org/10.1099/jgv.0.001020
18. National Center for Biotechnology Information. Pairwise Sequence Comparison (PASC) [cited 2021 Jul 10]. https://www.ncbi.nlm.nih.gov/sutils/pasc/viridty.cgi?textpage=overview
19. Price MN, Dehal PS, Arkin AP. FastTree 2—approximately maximum-likelihood trees for large alignments. PLoS One. 2010;5:e9490. https://doi.org/10.1371/journal.pone.0009490
20. Kumar S, Stecher G, Li M, Knyaz C, Tamura K. MEGA X: Molecular Evolutionary Genetics Analysis across computing platforms. Mol Biol Evol. 2018;35:1547–9. https://doi.org/10.1093/molbev/msy096
21. Ravasi D, De Respinis S, Wahli T. Multilocus sequence typing reveals clonality in *Saprolegnia parasitica* outbreaks. J Fish Dis. 2018;41:1653–65. https://doi.org/10.1111/jfd.12869
22. World Organisation for Animal Health. Aquatic | Manual online access [cited 2021 Jul 10]. https://www.oie.int/|standard-setting/aquatic-manual/access-online
23. Shi M, Lin X-D, Chen X, Tian J-H, Chen L-J, Li K, et al. The evolutionary history of vertebrate RNA viruses. Nature. 2018;556:197–202. https://doi.org/10.1038/s41586-018-0012-7
24. Hume AJ, Mühlberger E. Distinct genome replication and transcription strategies within the growing filovirus family. J Mol Biol. 2019;431:4290–320. https://doi.org/10.1016/j.jmb.2019.06.029
25. Barr JN, Weber F, Schmaljohn CS. *Bunyavirales*: the viruses and their replication. In: Howley PM, Knipe DM,

Whelan SPJ, editors. Fields virology. 7th ed. Philadelphia: Wolters Kluwer/Lippincott Williams & Wilkins; 2020. p. 706–49.

26. Lauber C, Gorbalenya AE. Partitioning the genetic diversity of a virus family: approach and evaluation through a case study of picornaviruses. J Virol. 2012;86:3890–904. https://doi.org/10.1128/JVI.07173-11
27. International Committee on Taxonomy of Viruses [cited 2021 Jul 10]. https://talk.ictvonline.org/taxonomy
28. Walker PJ, Siddell SG, Lefkowitz EJ, Mushegian AR, Adriaenssens EM, Alfenas-Zerbini P, et al. Changes to virus taxonomy and to the International Code of Virus Classification and Nomenclature ratified by the International Committee on Taxonomy of Viruses (2021). Arch Virol. 2021;166:2633–48. https://doi.org/10.1007/s00705-021-05156-1
29. Kibenge FSB, Godoy MG, editors. Aquaculture virology. Amsterdam: Elsevier; 2016. p. 568.
30. Geoghegan JL, Di Giallonardo F, Cousins K, Shi M, Williamson JE, Holmes EC. Hidden diversity and evolution of viruses in market fish. Virus Evol. 2018;4:vey031. https://doi.org/10.1093/ve/vey031
31. Geoghegan JL, Di Giallonardo F, Wille M, Ortiz-Baez AS, Costa VA, Ghaly T, et al. Virome composition in marine fish revealed by meta-transcriptomics. Virus Evol. 2021;7:veab005.
32. Kuhn JH, Adkins S, Alioto D, Alkhovsky SV, Amarasinghe GK, Anthony SJ, et al. 2021 taxonomic update for phylum *Negarnaviricota* (*Riboviria: Orthornavirae*), including the large orders *Bunyavirales* and *Mononegavirales*. Arch Virol. 2021 Aug 31 [Epub ahead of print]. https://doi.org/10.1007/s00705-021-05143-6
33. Kurath G, Stone D. Fish rhabdoviruses (*Rhabdoviridae*). In: Bamford D, Zuckerman M, editors. Encyclopedia of Virology. 4th ed. Amsterdam: Elsevier; 2021. p. 324–31.
34. LaPatra S, Misk E, al-Hussinee L, Lumsden JS. Rhabdoviruses of fish. In: Kibenge FSB, Godoy MG, editors. Aquaculture virology. Amsterdam: Elsevier; 2016. p. 276–97.
35. Kuhn JH, Amarasinghe GK, Perry DL. *Filoviridae*. In: Howley PM, Knipe DM, Whelan SPJ, editors. Fields virology. 7th ed. Philadelphia: Wolters Kluwer/Lippincott Williams & Wilkins; 2020. p. 449–503.
36. Kuhn JH, Charrel RN. Arthropod-borne and rodent-borne virus infections. In: Jameson JL, Fauci AS, Kasper DL, Hauser SL, Longo DL, Loscalzo J, editors. Harrison's principles of internal medicine. 20th ed. Columbus (OH): McGraw-Hill Education; 2018. p. 1489–509.

Address for correspondence: Torsten Seuberlich, Divison of Neurological Sciences, Vetsuisse Faculty, University of Bern, Bremgartenstrasse 109a, CH-3012 Bern, Switzerland; email: torsten.seuberlich@vetsuisse.unibe.ch

Article DOI: https://doi.org/10.3201/eid2712.210491

Four Filoviruses, 1 Hantavirus, and 1 Rhabdovirus in Freshwater Fish, Switzerland, 2017

Appendix

Methods

Bioinformatics

Reads were quality-trimmed using trimmomatic v. 0.36 (28), and host-derived sequences were removed by aligning reads to the European perch genome (UTU_Pfluv_1.1, Bioproject PRJNA450919) using STAR v. 2.6.0c (*1*). Non-aligned reads were assembled with SPAdes v. 3.12.0 (*2*). The resulting scaffolds were screened for homologies on the nucleotide and amino acid levels using BLASTn v. 2.7.1+ (*3*) against viral nucleotide sequences in GenBank (https://www.ncbi.nlm.nih.gov/genbank/) and DIAMOND v. 0.9.18 (*4*) and against viral protein sequences in UniProt (https://www.uniprot.org/), respectively. (Databases were downloaded on 20 May 2020.)

RT-PCR, RACE, Sanger sequencing

To fill gaps between HTS scaffolds, we reverse-transcribed extracted RNA to cDNA with SuperScript III Reverse Transcriptase (Thermo Fisher Scientific, Waltham, MA, USA) and performed PCR assays with Q5 Hot Start High-Fidelity DNA Polymerase (New England Biolabs, Ipswhich, MA, USA) and scaffold-specific primers (Appendix Table 3) according to the manufacturers' instructions. We gel-purified amplicons using the NucleoSpin Gel & PCR Clean-up Kit (Macherey-Nagel, Oensingen, Switzerland) and sequenced them using a 3730 DNA Analyzer (Thermo Fisher Scientific) with the BigDye Terminator v3.1 Cycle Sequencing Kit (Thermo Fisher Scientific), using standard protocols. We performed 3' and 5' RACE, as described previously on RNA extracted from pooled organs and CNS as well as cell culture supernatants (*5*). We purified RACE products and sequenced them as described above. Resultant data were analyzed with Geneious v 9.1.8 (Biomatters, Auckland, New Zealand).

In Situ hybridization (ISH)

We conducted chromogenic ISH on all of the FFPE tissues used for histopathology. Staining was performed with the RNAscope system (Advanced Cell Diagnostics, Newark, CA, USA). Using the RNAscope 2.5 HD Assay-Brown according to the manufacturer's instructions. ISH probes were designed by the company for EGLV (catalog #590061), BRPV (#590031), FIWIV (#590041), and OBLV (#590051). We counterstained slides with Mayer's hemalum solution (Merck KGaA, Darmstadt, Germany) and mounted them with Aquatex (Merck KGaA). Sections of apparently healthy European perch from a different origin, which we examined for a normal health control, served as negative controls. ISH process controls consisted of brain tissue sections of animals with bovine astrovirus CH13 (BoAstV CH13) infection and a BoAstV CH13-specific RNAscope probe [#406921] tested in parallel to each ISH experiment (*6*).

References

<jrn>1. Dobin A, Davis CA, Schlesinger F, Drenkow J, Zaleski C, Jha S, et al. STAR: ultrafast universal RNA-seq aligner. Bioinformatics. 2013;29:15–21. PubMed https://doi.org/10.1093/bioinformatics/bts635</jrn>

<jrn>2. Bankevich A, Nurk S, Antipov D, Gurevich AA, Dvorkin M, Kulikov AS, et al. SPAdes: a new genome assembly algorithm and its applications to single-cell sequencing. J Comput Biol. 2012;19:455–77. PubMed https://doi.org/10.1089/cmb.2012.0021</jrn>

<jrn>3. Camacho C, Coulouris G, Avagyan V, Ma N, Papadopoulos J, Bealer K, et al. BLAST+: architecture and applications. BMC Bioinformatics. 2009;10:421. PubMed https://doi.org/10.1186/1471-2105-10-421</jrn>

<jrn>4. Buchfink B, Xie C, Huson DH. Fast and sensitive protein alignment using DIAMOND. Nat Methods. 2015;12:59–60. PubMed https://doi.org/10.1038/nmeth.3176</jrn>

<jrn>5. Hierweger MM, Werder S, Seuberlich T. Parainfluenza virus 5 infection in neurological disease and encephalitis of cattle. Int J Mol Sci. 2020;21:498. PubMed https://doi.org/10.3390/ijms21020498</jrn>

<jrn>6. Küchler L, Rüfli I, Koch MC, Hierweger MM, Kauer RV, Boujon CL, et al. Astrovirus-associated polioencephalomyelitis in an alpaca. Viruses. 2020;13:50. PubMed https://doi.org/10.3390/v13010050</jrn>

Appendix Table 1. Results of the bioinformatics pipeline for virus discovery in samples from European perch*

	Scaffold			DIAMOND best protein hit	Amino acid alignment		
Virus family	ID	Length	kmer coverage	Accesssion number|protein|virus	Identity (%)	Length [nt]	Query covera
Hantaviridae	10	6509	3010	A0A2P1GNS4|Large protein|W. red spikefish virus	34.4	2104	94.8
	59	3784	11122	A0A2P1GNS8|Glycoprotein|W. minipizza batfish virus	25.4	836	63.1
	550	2160	15043	A0A2P1GNX7|Nucleoprotein|W. red spikefish virus	30.3	330	42.4
Rhabdoviridae	2058	1454	5.8	Q8UYI1|Nucleocapsid protein|sea trout rhabdovirus	42.3	267	54.8
	4052	1146	3	Q8UY99|Glycoprotein|lake trout rhabdovirus	87.5	80	97.2
	6439	960	5.7	Q8V316|Phosphoprotein|sea trout rhabdovirus	62.2	74	67.5
	8194	873	1.9	K7X7F6|Large protein|perch rhabdovirus	95.2	84	89.4
	10813	771	5.2	Q8V315|Matrix protein|sea trout rhabdovirus	94.8	213	82.9
	10889	768	1.9	A0A0A7|Large protein|eel virus European X	76.4	254	98.8
	12097	731	2.4	K7X7F6|Large protein|perch rhabdovirus	87.2	243	99.7
	37625	394	1	Q8V317|Large protein|lake trout rhabdovirus	93.2	426	87.9
	42117	370	2	K7X7F6|Large protein|perch rhabdovirus	89	354	92.7
	52025	331	1.4	Q8V317|Large protein|lake trout rhabdovirus	93.8	96	99.7
	52641	329	1.1	K7X7F6|Large protein|perch rhabdovirus	84.4	122	98.9
	68156	289	1.3	Q8UY99|Glycoprotein|lake trout rhabdovirus 903/87	77.6	303	94.7
	71803	282	0.96	Q8V313|Large protein|sea trout rhabdovirus	66.7	84	98.8
	89460	256	2.4	K7X7F67|Large sprotein|perch rhabdovirus	98.2	110	99.7
	90246	255	3.8	K7X7F6|Large protein|perch rhabdovirus	82.1	84	98.4
	97442	247	1.7	Q8V313|Polymerase protein |sea trout rhabdovirus	90.8	130	99
Filoviridae	4	14593	23.5	A0A2P1GMM1|Large protein|Huángjiāo virus	50.3	843	17.6
	5	13764	15.2	A0A2P1GMM1|Large protein|Huángjiāo virus	59.8	2145	46.5
	14†	10362	4.8	A0A2P1GMM1|Large protein|Huángjiāo virus	68	1471	42.5
	1005	3259	3	A0A2P1GMM1|Large protein|Huángjiāo virus	47.1	1089	99.9
	10054	3259	3	A0A2P1GMM1|Large protein|Huángjiāo virus	47.1	1089	99.9
	5282†	1945	4.1	A0A2P1GMM1|Large protein|Huángjiāo virus	41	648	99.6
	7085	1729	2.2	A0A2P1GMM5|Nucleoprotein|Huángjiāo virus	38.8	389	66.8
	11776	1389	1.8	A0A2P1GMM1|Large protein|Huángjiāo virus	41.6	334	71.7
	34171†	779	2.6	A0A2P1GMM5|Nucleoprotein|Huángjiāo virus	61.6	250	96.3
	50926	573	3	A0A2P1GMM1|Large protein|Huángjiāo virus	58.4	190	99.5
Other	1	10069	95	A0A1I9QNF6|Capsid protein|marbled eel polyomavirus	27.1	491	13.8
	201	2764	6.8	A0A1S7J028|LargeT|Rousettus aegyptiacus polyomavirus 1	28.6	255	26.6
	44589	359	0.7	A0A2P1GNG4|Polyprotein|Běihăi rabbitfish_calicivirus	57.4	115	95.3

*Abbreviations: W., Wēnlǐng; put, putative.
†These scaffolds were linked by RT-PCR resulting in the sequence of a novel virus here named Kander virus (KNDV).

Appendix Table 2. Comparison of conserved terminal sequences in genome segments of selected genera of the order *Bunyavirales**

Genus	3′ terminus	5′ terminus
Orthohantavirus	AUCAUCAUCUG...	...AUGAUGAU
Orthobunyavirus	**UCAUCA**CAUGA...	...UCGUG**UGAUGA**
Orthonairovirus	AGAGUUUCU...	...AGAAACUCU
Orthotospovirus	UCUCGUUAG...	...CUAACGAGA
Phlebovirus	UGUCGUUAG...	...CUAACGAGA
Actinovirus	**UCAUCA**UU...	...AA**UGAUGA**
(Species: Perch *actinovirus*, *Bunyavirales*)		

*Adapted from Barr JN, Weber F, Schmaljohn CS. Bunyavirales: the viruses and their replication. In: Howley PM, Knipe DM, Whelan SPJ, editors. Fields virology. 7th ed. Philadelphia, Pennsylvania, USA: Wolters Kluwer/Lippincott Williams & Wilkins; 2020. p. 706-49.

Appendix Table 3. Gene-specific primers for RT-PCRs, Sanger sequencing, and RACE

Name	Sequence	Comment
RT_FiloV_3140F	TGTGAGCTCACCAACCGTAC	Confirmation
RT_FiloV_3483R	GAGCCGTTTCTCCCAAGACA	Confirmation
RT_HantaV_2950F	CCCGGAAGTCCAGAACCTTC	confirmation
RT_HantaV_3269R	CGGTCAGGGAATCATCGGAG	confirmation
RT_RhabdoV_1064F	AAATGCCATTGCCAACACCG	confirmation
RT_RhabdoV_1370R	GTACGCTCCGACAGTGTCTT	confirmation
RT_HantaV_L_493R	AAACTGAAGCTCGATGCCCA	RACE
RT_HantaV_L_322R	CCAGCTGCCCAGGGAATATC	RACE
RT_HantaV_L_5998F	CGTCAGGTCCTGGATCAAGG	RACE
RT_HantaV_L_6190F	CTCCGCTGTGAACATGGTTG	RACE
RT_HantaV_M_541R	TTCTGCCGCCTTTCAAAGC	RACE
RT_HantaV_M_305R	CTCTTGGATCCTGGGTGTCG	RACE
RT_HantaV_M_3273F	ACATAGGCACTGTCCTCAAGC	RACE
RT_HantaV_M_3466F	TTCCGACGAGACCTCCTTCT	RACE
RT_HantaV_S_526R	CAGCCTGTGTTTCCGGAGTA	RACE
RT_HantaV_S_281R	GCTGGATCTGAAGGCAGGAG	RACE
RT_HantaV_S_1656F	CCCAAACAGGTCGGTCATCA	RACE
RT_HantaV_S_1848F	CAAGGTGGTCTCCATGGGG	RACE
RT_RhabdoV_1335F	ATCCAACATGCCCGCAAAGA	connection of contigs
RT_RhabdoV_1684R	TCCCAGCTCCACTAATCCCT	connection of contigs
RT_RhabdoV_2391F	GAATGGAATGGATGCCAGCG	connection of contigs
RT_RhabdoV_2863R	GCCACGACCATCGCATTTTT	connection of contigs
RT_RhabdoV_3358F	GCAATGAGAAAGTGCTGAACCA	connection of contigs
RT_RhabdoV_3750R	CCCATGCCGCAGTTTGATAC	connection of contigs
RT_RhabdoV_3765F	GTAGAGGGGAAGTTGTGCGT	connection of contigs
RT_RhabdoV_4214R	CTGCTGTCGAACGATTGCAC	connection of contigs
RT_RhabdoV_5913F	GTTGGGCGTATGCAGACTCT	connection of contigs
RT_RhabdoV_6225R	GCTCTGCGTTGACAAAGTCA	connection of contigs
RT_RhabdoV_6256F	GATCTTTTCGGCATTGGGGC	connection of contigs
RT_RhabdoV_6559R	TCGAAGATTTTGGTCAGAGGCA	connection of contigs
RT_RhabdoV_6636F	CATGTAGAACGACGGCCCTT	connection of contigs
RT_RhabdoV_7823R	TCCTCGAATTGCCGGATTGT	connection of contigs
RT_RhabdoV_7793F	AGTAGAGTTTCACAATCCGGCA	connection of contigs
RT_RhabdoV_8342R	CAGCGATATCAGGGATTCGGT	connection of contigs
RT_RhabdoV_8780F	GCTGAGAGCCGCTATCACAT	connection of contigs
RT_RhabdoV_9479R	GGACAACGCAGATGCCTTGA	connection of contigs
RT_RhabdoV_10828F	GAGGCTCGACAGGGATCAAG	connection of contigs
RT_RhabdoV_11124R	TCTTCTCCCCTTTGCAACTGA	connection of contigs
RT_Rhabdo_6952F	AGGAGTCAAGGGCAAGGAGA	connection of contigs
RT_Rhabdo_7555R	GCTGACTGGATTGTCTCGTCA	connection of contigs
RT_Rhabdo_6980F	ACGAGCACATCAGTATTGCCA	connection of contigs
RT_Rhabdo_575R	CTCGTTTTGGATCCCCACGA	RACE
RT_Rhabdo_330R	CCAATTCGCTCGGCAATCTG	RACE
RT_Rhabdo_11050F	CGAATCTCTGCTTGCAGTGC	RACE
RT_Rhabdo_11222F	AGGAAGATGGCCACCATTGG	RACE
P_FiloV_13to3360_1435F	CACAGTGGTAAGGGCCATGA	connection of contigs
P_FiloV_13to3360_1884R	CCGGTGTCAACGGCTGTTAT	connection of contigs
P_FiloV_13to5716_12038F	GTCTGCATAGGGAAGGTGGC	connection of contigs
P_FiloV_13to5716_12590R	CTTGTCGCTCCTGAAGACGT	connection of contigs
Perch_FiloV2_296R	TTGCAAGAATGAAGGCACACC	RACE
Perch_FiloV2_511R	AAACCTTGCGGCTTGATTGG	RACE
Perch_FiloV2_14328F	ACGCCTTGGTCAAATCCACA	RACE
Perch_FiloV2_14118F	TTGCTCTTGTGGCAGCAGAA	RACE

Name	Sequence	Comment
Perch_FiloV1_260R	GTCGACTGAGTTGTCTCCCC	RACE
Perch_FiloV1_455R	GTATGGTAATGCCGTTGGTGC	RACE
Perch_FiloV1_13492F	TCCTAGGGAGTCTGCAGAGG	RACE
Perch_FiloV1_13275F	GACAGGTCCGGAGTGAAGTC	RACE

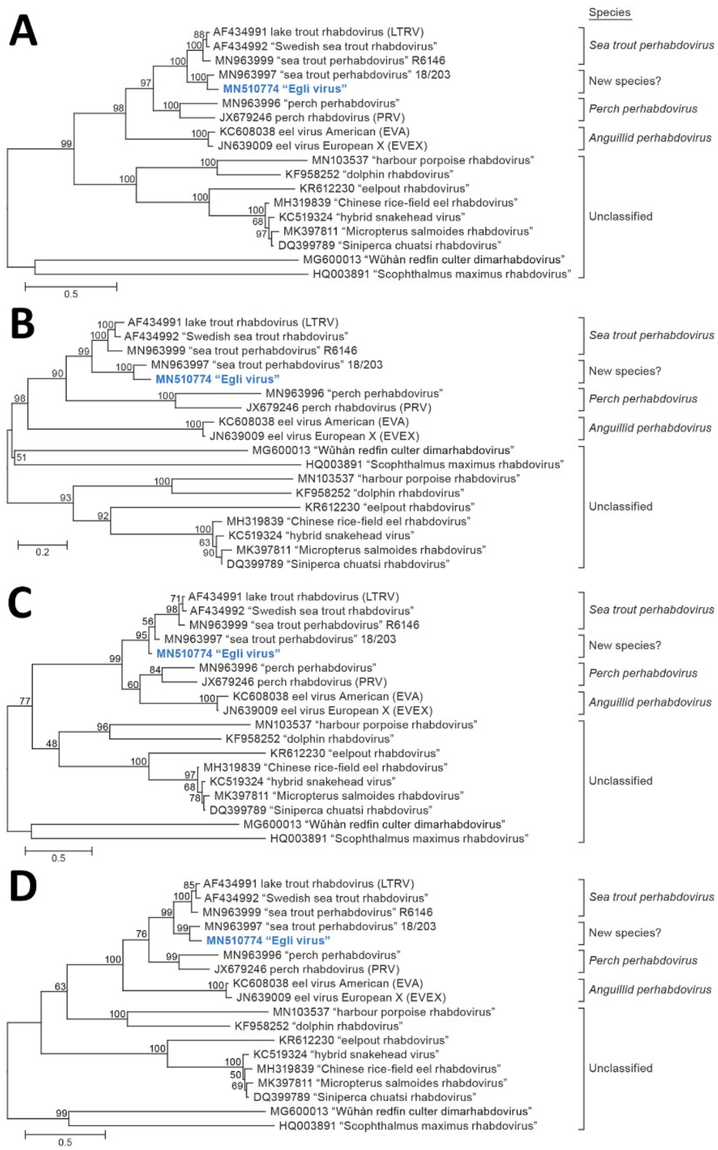

Appendix Figure 1. Maximum-likelihood phylogenetic trees of the nucleotide sequences of Egli virus (EGLV; bold blue) genes with those of viruses belonging to representative members of the genus *Perhabdovirus*. a) nucleoprotein gene (*N*), b) phosphoprotein gene (*P*) c) matrix protein gene (*M*), and d) glycoprotein gene (*G*). Numbers near nodes on the trees indicate bootstrap values. Branches are labeled by GenBank accession number, virus name, and virus name abbreviation in parenthesis. The names of unclassified, likely perhabdoviruses are placed in quotation marks and printed without name abbreviations. The scale (bottom left) indicates the number of substitutions per site, reflected by the branch lengths.

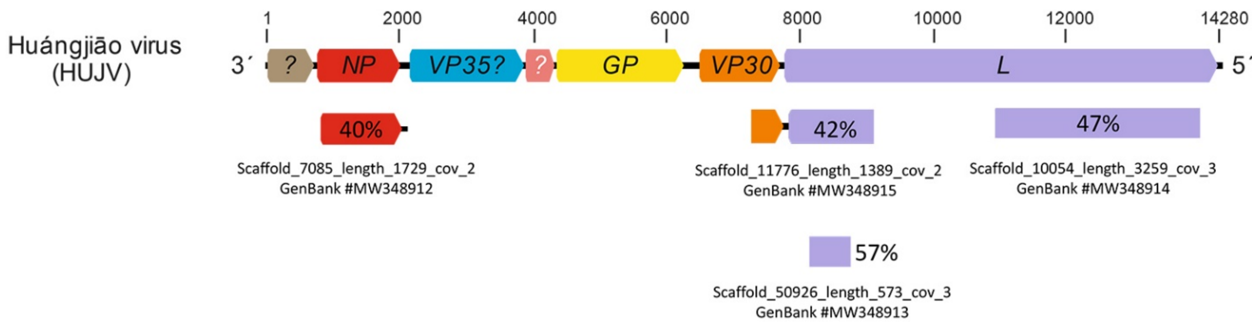

Appendix Figure 2. Mapping of additional scaffolds identified in European perch with hits to Huángjiāo virus (HUJV). The HUJV genome organization is shown schematically on the top and allocated scaffolds (scaffold IDs [shortened] and GenBank accession numbers) to the genomic regions of the encoded proteins with respective hits and their identity at the amino-acid sequence level. Open reading frames (ORFs) are indicated as colored arrows. ORFs encoding HUJV-like proteins (indicated as percentages) are depicted by the same color. *NP*, nucleoprotein gene; *VP35*, polymerase cofactor gene; *GP*, glycoprotein gene; *VP30*, transcriptional activator gene; *L*, large protein gene. Question marks indicate novel ORFs.

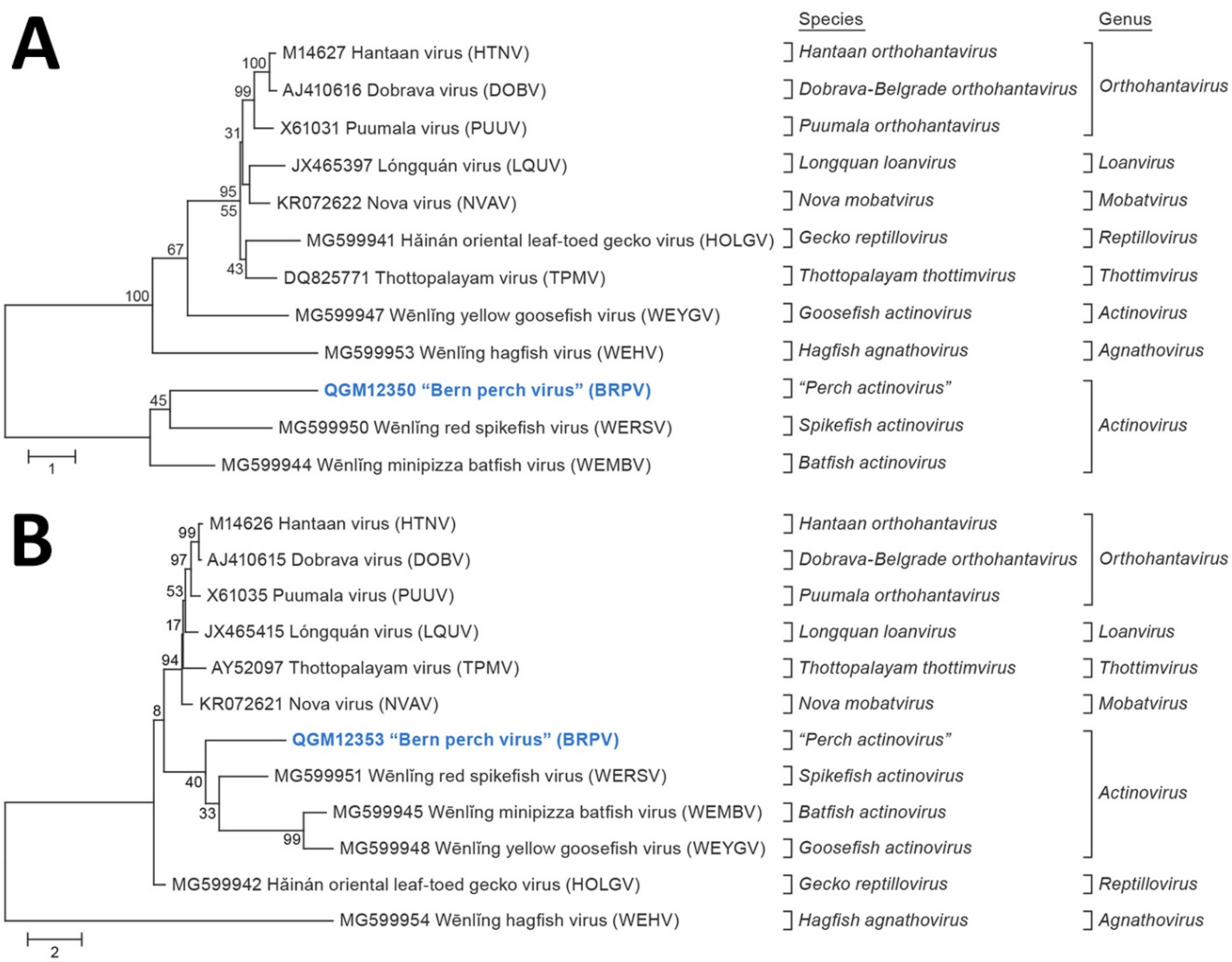

Appendix Figure 3. Maximum-likelihood phylogenetic trees of amino-acid sequences of Bern perch virus (BRPV; bold blue) structural proteins with those of viruses belonging to representative members of the family *Hantaviridae*. a) Glycoprotein precursor (GPC), encoded by the M segment, b) nucleocapsid protein, encoded by the S segment. Numbers near nodes on the trees indicate bootstrap values. Branches are labeled by GenBank accession number, virus name, and virus name abbreviation in parenthesis. Unclassified, likely hantaviruses and officially proposed hantavirus species names are placed in quotation marks. The scale (bottom left) indicates the number of substitutions per site, reflected by the branch lengths.

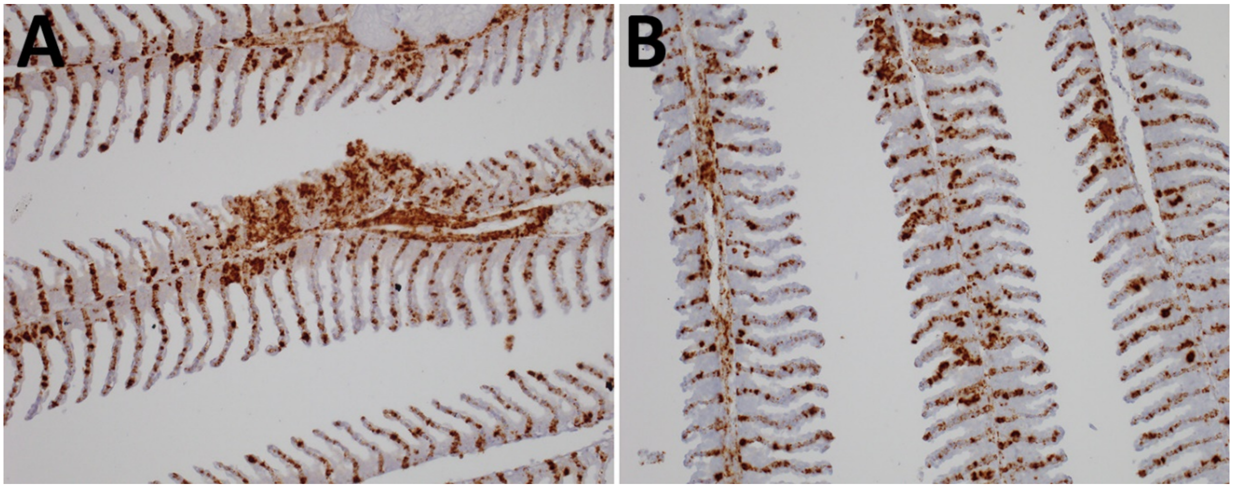

Appendix Figure 4. Detection of Bern perch virus (BRPV) genomic RNA in gills of two individual European perch (A, B) by in situ hybridization (brown labeling).